3D Dynamic Simulation of a Metal Hydride-Based Hydrogen Storage Tank

A. Freni*, F. Cipitì
CNR- Institute for Advanced Energy Technologies "Nicola Giordano", Via S. Lucia sopra Contesse n. 5, 98126 Messina, Italy
*Corresponding author: e-mail: angelo.freni@itae.cnr.it

Abstract: In this paper a 3D dynamic simulation for a portion of a metal hydrides-based ($LaNi_5$) hydrogen storage tank is presented. The model is based on heat and mass balances and considers coupled heat and mass transfer resistance through a non-uniform pressure and temperature sorbent bed. The governing equations were implemented and solved using COMSOL Multiphysics software package. The simulation results showed that the most relevant parameters for the optimization design of the metal hydrides tank are the hydrogen charge pressure, the permeability and the thermal conductivity of the metal hydride sorbent bed.

Keywords: hydrogen storage, modeling, metal hydrides

1. Introduction

Storage is a key factor in the development of the hydrogen economy, in particular for the transport sector [1]. "On-board" hydrogen storage requires a safety and efficient technology, compatible with vehicle requirements. Among different storage methodologies, the reversible sorption of hydrogen on metal hydrides appears to be particularly interesting [2]. AB5 intermetallic compounds and especially LaNi5 metal hydride, are considered very promising for these applications, due to a high storage volumetric density, and operating conditions of pressure and temperature compatible with Fuel Cells (T=20-60°C, P=1-10 bar) [3]. A metal hydride-based hydrogen storage tank is more compact and safe in comparison with traditional pressurized tanks. The U.S. Department of Energy (DOE) has established, in the framework of DOE Hydrogen Program, some parameters that represent the technological targets for developing efficient on-board hydrogen storage tank. Among these, particularly restrictive is the tank fill time that must be below 10 minutes, considering a stored hydrogen mass of 5 kg [4]. For this reason, one of the most investigated subject in literature is the development of tanks able to efficiently provide/remove thermal energy during the hydrogen charge/discharge. Different mathematical models have been proposed in literature aimed at designing hydrogen storage tank with high thermal exchange properties. Some models have been proposed focusing on the description of chemical-physics processes that occur on hydride bed during hydrogen charge phase. However such mono-bi dimensional models describe simplified tank geometry [5-11] and can not be used to design tanks with complex architecture.

In this paper, a 3-dimensional reactor configuration has been simulated, consisting of some parallel tubes (where the cooling/heating fluid flows) across a cylindrical LaNi5-based hydrogen storage tank.

Mathematical simulations have been achieved though the description of transport phenomena by partial differential equations (PDEs), using Comsol Multiphysics. The main advantage of this finite-element approach is the possibility to easily adapt the model to different reactor geometry, allowing an accurate design. In the first part of the paper, the governing equations of the model have been introduced. In the second part, the simulation results of a base-case and, subsequently, the results of a parametric analysis aimed at identifying the key factors to optimize the reactor geometry, have been reported.

2. Numerical Model

Fig. 1 shows the geometry of the implemented rector portion. The adsorbent bed is a cylinder filled with commercial LaNi5 grains, where some tubes (with the cooling/heating fluid water flowing) cross through. Hydrogen enters in the reactor axial direction. The main geometrical and thermal-physical parameters are reported on Tab. I.

The main assumptions considered in developing the model are the following:

a) The media is in local thermal equilibrium (gas temperature is the same of solid temperature).

b) The solid phase is isotropic and has an uniform porosity.

c) The gas phase is ideal, from a thermodynamic point of view.

d) Equilibrium gas pressure is calculated by Van't Hoff equation, neglecting hysteresis and plateau inclination of the real pressure/concentration isotherms.

e) Thermal-physical properties are constant.

f) The system is adiabatic.

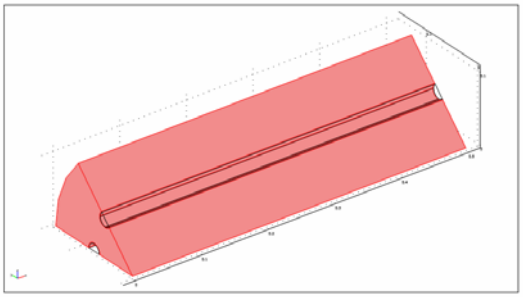

Figure 1. Reactor portion geometry implemented on Comsol Multiphysics software.

The governing equations consist of energy balances for heating/cooling fluid, heat exchanger metal, hydride bed, and mass balances for hydrogen diffusion. The model describes hydrogen diffusion through hydride bed using the Darcy's law [12] and taking into consideration the kinetics of the adsorption as a function of the difference between the local and the equilibrium pressure [13].

Based on these considerations, the following equations have been considered:

Energy balances for heating/cooling fluid:

$$\rho_f c_{pf} \frac{\partial T_f}{\partial t} + \nabla \cdot \left(-\lambda_f \nabla T_f\right) = 0 \tag{1}$$

Energy balances for heat exchanger metal:

$$\rho_m c_{pm} \frac{\partial T_m}{\partial t} + \nabla \cdot \left(-\lambda_m \nabla T_m\right) = 0 \tag{2}$$

Energy balances for hydride bed:

$$\left[(1-\varepsilon)\rho_s c_{ps} + \varepsilon \rho_g c_{pg}\right] \frac{\partial T_s}{\partial t} + \nabla \cdot \left(-\lambda_s \nabla T_s\right) + \\ + \nabla \cdot \left(\rho_g c_{pg} \vec{u} T_s\right) = (1-\varepsilon) |\Delta H| \frac{\partial \rho_s}{\partial t} \tag{3}$$

Mass balances for hydride bed:

$$\varepsilon \frac{\partial \rho_g}{\partial t} + \nabla \cdot \left(\vec{u} \rho_g\right) = -(1-\varepsilon) \frac{\partial \rho_s}{\partial t} \tag{4}$$

Moreover, the following additional equations have been considered:

Perfect gas law

$$\rho_g = \frac{M_g P}{R T} \tag{5}$$

Darcy's law

$$\vec{u} = -\frac{K}{\mu_g} \nabla p \tag{6}$$

Kozeny – Carman's equation

$$K = \frac{d_p^2 \varepsilon^3}{150 \cdot (1-\varepsilon)^2} \tag{7}$$

Adsorption kinetics

$$\frac{\partial \rho_s}{\partial t} = C_a \exp\left(-\frac{E_a}{R T}\right) ln\left(\frac{P}{P_{eq}}\right) (\rho_{ss} - \rho_s) \tag{8}$$

Van't Hoff's law

$$P_{eq} = exp\left(A - \frac{B}{T}\right) \tag{9}$$

In paricular, Eq. (5) determines the gas density, considering the assumption c). Eq. (6) il the well known with the Darcy's law. Eq. (7) estimates the sorption bed permeability with the Kozeny – Carman law [14]. Eq. (8) describes the reaction kinetics, where the constant Ca depends on the type of hydride; the values of the

activation energy Ea for the LaNi5–hydrogen system are reported in literature [15]. Eq. (9) calculates the equilibrium pressure with the Van't Hoff's law; A and B coefficients depend on hydride considered [16].

The initial and boundary conditions are the following:

Initial conditions:

$$T_f = T_m = T_s = T_0 ; p = p_0 ; \quad \rho = f(p_0, T_0)$$

Boundary conditions:

$$T_f\big|_{z=0} = T_{cool}$$

where T_{cool} denotes the inlet temperature of the cooling fluid.

$$-\lambda_s \frac{\partial T_m}{\partial r}\bigg|_{r=rm} = h_w (T_m - T_s)$$

where h_w denotes the thermal resistance at the interface metal-hydride (r_m = external radius of metal tubes)

$$p\big|_{z=0} = p_{ext}$$

where $p_{ext} > p_0$ denotes the inlet hydrogen pressure.

The other boundary conditions (not showed) are thermal insulations, or symmetry.

3. Results

3.1 Base case

The main input data used in the base-case are reported in Tab. I. The simulated process is the charge phase, considering an inlet pressure of 8 atm. The inlet temperature of the cooling fluid is at a constant temperature of 20°C. The tank is considered initially at a temperature of 20°C and a pressure of 1.5 atm. The permeability K of the hydride bed, for this base case, is $1e^{-12}$ m^2.

Tab. 1: Input data for the model (base-case)

Parameter	Symbol	Value
External radius of the hydrides bed	R_e	0.1 m
Length of the hydrides bed	L	0.5 m
External radius of metal tubes	r_m	0.1 m
Number of heat exchange tubes	N	8
Velocity of heating/cooling fluid	v	0.5 m s^{-1}
Initial temperature	T_o	20 °C
Initial pressure	p_o	1.5 atm
Initial hydride density	ρ_o	3200 kg m^{-3}
Saturation hydride density	ρ_{ss}	3240 kg m^{-3}
Porosity of the hydrides bed	ε	0.5
Hydride specific heat	C_{ps}	419 J kg^{-1} K^{-1}
Hydride thermal conductivity	k_s	1.2 W m^{-1} K^{-1}
Sorption enthalpy	ΔH	30800 J mol^{-1}
Wall heat transfer coefficient at the interface heat exchanger - hydride	h_w	1650 W m^{-2} K^{-1}
Hydrogen charge pressure	p_{ext}	8 atm
Temperature of cooling fluid	T_{cool}	20 °C

Fig. 2 shows the 3D distribution of the temperature at t=1000 sec. The heating of the hydride bed, due to the exothermic process of hydrogen sorption is clearly evidenced. Moreover, it can be seen that the bed portion near the cooling tubes has a lower temperature than the outer zones.

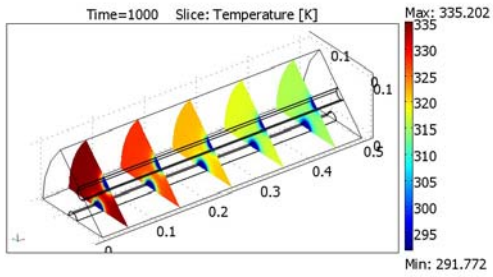

Figure 2. Reactor temperature distribution at a simulation time t=1,000 sec

Fig. 3a, b, c show slice distributions of the hydride temperature, pressure and density in the reactor section z=0.25 m. Fig. 3a shows that the outer area of the hydride bed reaches a maximum temperature of 60°C. This increase is less evident near the tubes, due to the temperature T_f of the cooling fluid. In Fig. 3b is shown that the pressure after 1000 sec reaches the maximum value of 8 atm, that is the inlet pressure of hydrogen. Fig. 3c reports the slice distribution of hydride density, showing an homogeneous

distribution of the sorbed hydrogen. The calculated density is about 3,239 kg m^{-3}, near to the saturation density ρ_{so} =3240 kg m^{-3}, showing that, after 1,000 sec, the reactor has almost completed the charge phase of hydrogen.

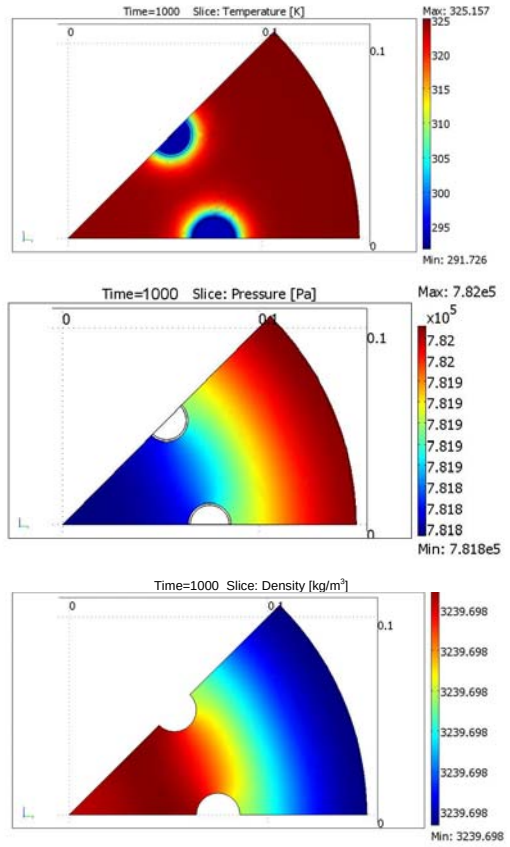

Figure 3a, b, c: Slice distributions (x-y plane) of hydride temperature, pressure and density (z=0.25 m, t=1000 sec).

The profiles of average temperature, pressure and density of the hydride bed, as a function of time, are reported on Fig. 4a, b. Fig. 4a shows for the base-case that the system reaches rapidly the maximum temperature of 63 °C, starting from 20 °C. After this rapid increase, the temperature decreases, till the average temperature reaches the temperature of the cooling fluid (20 °C) after about one hour.. Cooling time for the simulated reactor is quite high due to the low conductibility of the hydride bed and the not optimized thermal exchange.

Pressure distribution as a function of time is reported on Fig. 4b, starting from an initial value of 1.5 atm up to 8 atm, that is the inlet hydrogen pressure. Hydride density , increases, starting from an initial value of 3,200 kg m^{-3} up to ,240 kg m^{-3}, after about 1300 sec., in correspondance of the maximum hydrogen sorption, 1.3% weight.

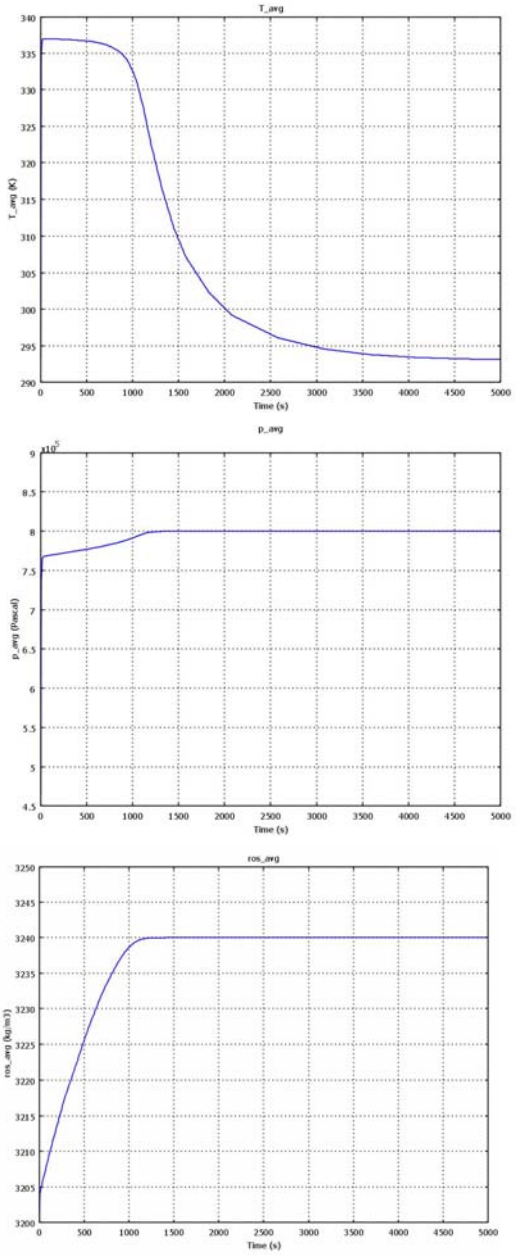

Figure 4a, b, c: Distribution of average values of temperature, pressure and density of the hydride bed as a function of time.

Based on the simulation results for the base-case, the following considerations can be derived: the saturation time, namely the time needed for the full hydrogen sorption, is about 1,300 sec; the maximum temperature is about 63 °C. Both the parameters must be as low as possible in order to optimize the filling phase. As a consequence, a sensitivity analysis has been carried out aimed at evaluating the effects of some critical parameters on the saturation time and the maximum temperature.

3.2 Sensitivity Analysis

A sensitivity analysis has been carried out in order to examine the influence of hydrogen inlet pressure, thermal conductivity of hydride bed, and permeability on saturation time. Fig. 5 shows the profile of the saturation time as a function of the inlet gas pressure for different values of permeability.

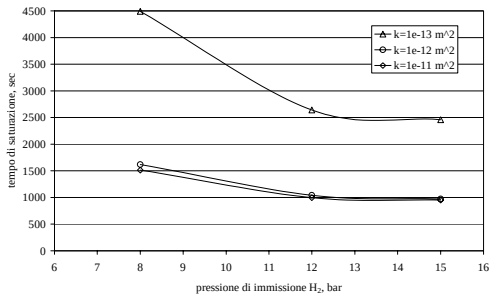

Figure 5: Saturation time profile as a function of inlet gas pressure for different values of permeability.

The gas permeability influences the results, since this parameter controls the mass transport. When this parameter decreases, gas velocity through matrix solid reduces, on the basis of Darcy's law (Eq. 6), increasing saturation time. Below a permeability of $K=1e^{-13}$ m^2, the system shows a decrease of performance. When the permeability is enough high ($K>1e^{-12}$ m^2), the low efficiency of heat exchange is the limiting factor of the process, therefore the system is not sensible at permeability variations. For lower values of the permeability, ($K<1e^{-13}$ m^2), the resistance at the hydrogen transport becomes the limiting factor. Moreover, it is shown how an increase of the inlet gas pressure implies a sensible decrease of the saturation time. In fact, increasing the charge pressure, the sorption kinetics (Eq. 8) improves. Fig. 6 shows the influence of the thermal conductivity for the hydride bed on the saturation time, for different values of permeability (charge pressure of 8 atm).

As expected, a high thermal conductivity for the hydride bed implies a decrease of the saturation time. An high thermal conductivity determines a decrease of the hydride bed temperature, favoring the sorption process. The sensitivity analysis, even if simplified and partial, pointed out that, for an adequate pressure charge and a high thermal conductivity of the hydride bed, a saturation time close to the target fixed by DOE (10 minutes) can be obtained. As a consequence, further research efforts should be focused on the improvement of the thermal exchange for the storage tank through the development of innovative hydride beds that, for example, with the adoption of graphite matrix or metallic foam, have enough hydrogen permeability and high equivalent thermal conductivity.

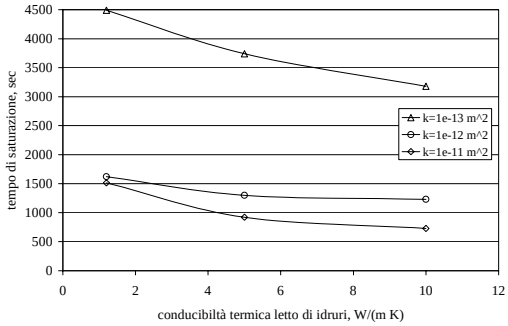

Figure 6: Saturation time profile as a function of the hydride bed for different values of permeability.

Future investigation will be focused on a parametric analysis to evaluate the influence of other parameters, such as thermal exchange surface, heat exchanger geometry, metal used for the heat exchanger and different metal hydrides with a higher hydrogen adsorption than the common LaNi5.

4. Conclusions

In this paper simulation results for a portion of a LaNi5 hydride-based hydrogen storage tank have been presented. The influence of the key parameters on the dynamic behavior of the system have been carried out by a sensitivity analysis for a base-case. Results show that the hydrogen charge pressure, the permeability and the thermal conductivity of the hydride bed are crucial factors for an optimized tank design.

5. References

[1] D.K. Ross, "Hydrogen storage: The major technological barrier to the development of hydrogen fuel cell cars", Vacuum 80 (2006) 1084–1089.

[2] B. Sakintunaa, F. Lamari-Darkrimb, M. Hirscherc, "Metal hydride materials for solid hydrogen storage:A review", International Journal of Hydrogen Energy 32 (2007) 1121–1140.

[3] S. Srivastava, O.N. Srivastava, "Hydrogenation behaviour with regard to storage capacity, kinetics, stability and thermodynamic behaviour of hydrogen storage composite alloys, $LaNi_5/La_2Ni_7$, $LaNi_3$", Journal of Alloys and Compounds, 290 (1999) 250–256.

[4] S. Satyapal, J. Petrovic, C. Read, G. Thomas, G. Ordaz, "The U.S. Department of Energy's National Hydrogen Storage Project: Progress towards meeting hydrogen-powered vehicle requirement", Catalysis Today 120 (2007) 246–256.

[5] T. Nakagawa, A. Inomata, H. Aoki, T. Miura, "Numerical analysis of heat and mass transfer characteristics in the metal hydride bed", Int. J. Hydrogen Energy, Vol. 25, pp. 339-350, 2000.

[6] M.Y. Ha, I.K. Kim, H.D. Song, S. Sung, D.H. Lee, "A numerical study of thermo-fluid phenomena in metal hydride beds in the hydriding process", Int. J. of Heat and Mass Transfer, 47 (2004), 2901-2912.

[7] E.S. Kikkinides, M.C. Georgiadis, A.K, Stubos. "On the optimization of hydrogen storage in metal hydride beds" Int J Hydrogen Energy, 31 (2006), 737–751.

[8] A. Jemni, S.Ben Nasrallah, "Study of two-dimensional heat and mass transfer during absorption in a metal-hydrogen reactor", Int. J. Hydrogen Energy, 20 (1995), 43-52.

[9] Kemal Aldas, Mahmut D. Mat, Yuksel Kaplan, "A three-dimensional mathematical model for absorption in a metal hydride bed", Int. J. Hydrogen Energy, 27 (2002), 1049-1056.

[10] P. Marty, J. F. Fourmigue, P. De Rango , D. Fruchart, J. Charbonnier, "Numerical simulation of heat and mass transfer during the absorption of hydrogen in a magnesium hydride", Energy Conversion and Management 47 (2006) 3632–3643.

[11] K. Nakaso, R. Shigenaga, J. Fukai, "Effect of heat transfer enhancement on energy release from a metal hydride tank", Journal of Chem. Eng. of Japan, 40 (2007), 1257-1263.

[12] D. M. Ruthven, "Principles of adsorption and adsorption process", J. Wiley & Sons, London (1984).

[13] H. Dhaoua, F. Askria, M. Ben Salaha, A. Jemnia, S. Ben Nasrallaha, J. Lamloumib, "Measurement and modelling of kinetics of hydrogen sorption by LaNi5 and two related pseudobinary compounds", International Journal of Hydrogen Energy 32 (2007) 576 – 587.

[14] R. B. Bird, W. E. Stewart and E. L. Lightfoot, Fenomeni di trasporto, Ambrosiana, Milan (1970).

[15] S. Suda, N. Kobayashi, Y. Yoshida, "Reaction kinetics of metal hydrides and their mixtures", J. Less-Common Metals, 73 (1980), 119-126.

[16] Hydride Properties Database, US Department of Energy's Sandia National Laboratories, http://hydpark.ca.sandia.gov/

[17] S.Ben Nasrallah, A. Jemni, "Heat and mass transfer models in metal-hydrogen reactor", Int. J. Hydrogen Energy, 22 (1997), 67-76.

[18] M. Martin, C.Gommel, C. Borkhart, E. Fromm, "Absorption and desorption kinetics of hydrogen storage alloys", Int Journal of Alloys and Compounds, 238 (1996) 193-2

6. Acknowledgements

This work has been financially supported by MIUR-FIRB Idee progettuali DM25768.

7. Nomenclature

A, B	Coeff. for calcuation of equilibrium pessure by eq. (9)
Ca	Coeff. for calculation of sorption kinetics by eq. (8), sec^{-1}
cp	Specific heat, J kg^{-1} K^{-1}

d_p	particle size, m
Ea	Activation Energy, J mol^{-1}
h_w	Wall heat transfer coefficient at the interface heat exchanger - hydride, W m^{-2} K^{-1}
K	Permeability, m^2
L	Length of the hydrides bed, m
Mg	Molecular weight kg mol^{-1}
p	Pressure, Pa
p_{ext}	Hydrogen charge pressure, Pa
R	Gas Constant, 8.314 J mol^{-1} K^{-1}
R_e	External radius of the hydrides bed, m
r_m	External radius of the metal tubes, m
t	Time, sec
T	Temperature, K
u	Gas velocity, m sec^{-1}

Greek symbols:

ΔH	Entahlpy, J kg^{-1}
ε	Porosity
λ	Thermal conductivitya, W m^{-1} K^{-1}
μg	Dynamic viscosity, kg m-1 sec-1
ρ	Density, kg m^{-3}

Subscripta:

eq	Equilibrium
f	Cooling fluid
g	Gas
m	Metal
o	Initial
s	Hydride
ss	Saturation